Molecular Biology of the Cell
Vol. 14, 4181–4195, October 2003

Yeast Kinetochores Do Not Stabilize Stu2p-dependent Spindle Microtubule Dynamics[V]

Chad G. Pearson,* Paul S. Maddox, Ted R. Zarzar, E.D. Salmon, and Kerry Bloom

Department of Biology, University of North Carolina at Chapel Hill, Chapel Hill, North Carolina 27599-3280

Submitted March 27, 2003; Revised June 14, 2003; Accepted June 14, 2003
Monitoring Editor: Trisha Davis

The interaction of kinetochores with dynamic microtubules during mitosis is essential for proper centromere motility, congression to the metaphase plate, and subsequent anaphase chromosome segregation. Budding yeast has been critical in the discovery of proteins necessary for this interaction. However, the molecular mechanism for microtubule–kinetochore interactions remains poorly understood. Using live cell imaging and mutations affecting microtubule binding proteins and kinetochore function, we identify a regulatory mechanism for spindle microtubule dynamics involving Stu2p and the core kinetochore component, Ndc10p. Depleting cells of the microtubule binding protein Stu2p reduces kinetochore microtubule dynamics. Centromeres remain under tension but lack motility. Thus, normal microtubule dynamics are not required to maintain tension at the centromere. Loss of the kinetochore (*ndc10-1*, *ndc10-2*, and *ctf13-30*) does not drastically affect spindle microtubule turnover, indicating that Stu2p, not the kinetochore, is the foremost governor of microtubule dynamics. Disruption of kinetochore function with *ndc10-1* does not affect the decrease in microtubule turnover in *stu2* mutants, suggesting that the kinetochore is not required for microtubule stabilization. Remarkably, a partial kinetochore defect (*ndc10-2*) suppresses the decreased spindle microtubule turnover in the absence of Stu2p. These results indicate that Stu2p and Ndc10p differentially function in controlling kinetochore microtubule dynamics necessary for centromere movements.

INTRODUCTION

Accurate segregation of the duplicated genome during cell division requires the mechanical separation of chromosomes to the daughter cells. The microtubule-based mitotic spindle provides the structural and mechanical framework, whereas protein/DNA structures (kinetochores) on chromosomes facilitate attachment to microtubules. Dynamically growing and shortening spindle microtubules nucleated from spindle poles gain attachment of their plus-ends to the kinetochore (Rieder and Salmon, 1998; Kapoor and Compton, 2002). Kinetochores maintain "end-on" attachment to a bundle of microtubules (kinetochore microtubules), producing tension between sister chromatids. Dynamic microtubules produce forces necessary for chromosome movement to facilitate congression to the spindle equator, oscillations at the metaphase plate, and chromosome segregation (Inoue and Salmon, 1995; Dogterom and Yurke, 1997; Rieder and Salmon, 1998; McIntosh *et al*., 2002; Scholey *et al*., 2003). Microtubule–kinetochore interactions serve to produce the primary force on chromosomes that, in concert with nonkinetochore forces (polar ejection forces and resistance between sister chromatids), result in dynamic chromosome behavior essential for proper cell division (Nicklas, 1989; Mitchison and Salmon, 1992; Skibbens *et al*., 1993; Murray and Mitchison, 1994; Khodjakov *et al*., 1999). Furthermore, dynamic instability of microtubule plus-ends and poleward flux contribute to the turnover of kinetochore microtubules in tissue cells (Mitchison, 1989). In vitro and in vivo studies have shown that attachment of microtubules to kinetochores generates stable microtubules compared with unattached spindle microtubules (Mitchison *et al*., 1986; Zhai *et al*., 1995; Hunt and McIntosh, 1998). This difference in microtubule growth and shortening upon kinetochore attachment indicates that, in tissue cells, microtubule dynamics is stabilized at the level of the kinetochore. The regulation of kinetochore microtubule dynamics is therefore critical for chromosome segregation and likely to involve the coordination of inherent dynamic properties of the microtubule polymer and microtubule-associated proteins.

Saccharomyces cerevisiae is a genetically tractable organism to study this complex process (Winey and O'Toole, 2001). The mitotic spindle structure in haploid cells consists of ~40 microtubules: eight overlapping interpolar microtubules and 32 kinetochore microtubules (Winey *et al*., 1995; O'Toole *et al*., 1999). This ultrastructural information combined with live cell analysis indicates that each kinetochore makes a persistent attachment to a single microtubule (Winey *et al*., 1995; O'Toole *et al*., 1999; Goshima and Yanagida, 2000; Goshima and Yanagida, 2001; Pearson *et al*., 2001). Before anaphase, kinetochores and spindle microtubules generate forces to separate sister centromeres toward their respective spindle poles, whereas chromosome arms maintain cohesion along their length. Centromere separation is dependent upon spindle microtubules and a functional kinetochore (Goshima and Yanagida, 2000; He *et al*., 2000; Tanaka *et al*.,

Article published online ahead of print. Mol. Biol. Cell 10.1091/mbc.E03–03–0180. Article and publication date are available at www.molbiolcell.org/cgi/doi/10.1091/mbc.E03–03–0180.

[V] Online version of this article contains video material for some figures. Online version is available at www.molbiolcell.org.

* Corresponding author. E-mail address: cgpearso@email.unc.edu.

Table 1. S. cerevisiae strains and plasmids

Strain name	Relevant genotype	Source/Reference
YEF473A	MATa *trp1-63 leu2-1 ura3-52 his3-200 lys2-801*	Pringle
GT1	MATa *trp1-63 leu2-1 ura3-52 his3-200 lys2-801 ura3-52::GFP-TUB1-URA3*	Maddox et al (2000)
KBY2012	MATa *trp1-63 leu2-1 ura3-52 his3-200 lys2-801 cse4::HYG SPC29-CFP-KAN* pKK1	This study
Y170	MATa *Ace1-UBR1 Ace1-ROX1 trp1Δ ade2-101 ura3-52 lys2-801 stu2Δ::URA3::Panb1UB-R-STU2 pTUB1-GFP-TUB1*	Kosco/Huffaker
KBY2660.291	MATa *Ace1-UBR1 Ace1-ROX1 trp1Δ ade2-101 ura3-52 lys2-801 stu2Δ::URA3::Panb1UB-R-STU2 cse4::HYG SPC29-CFP-KAN* pKK1	This study
KBY2665	MATa *trp1-63 leu2-1 ura3-52 his3-200 lys2-801 ura3-52::GFP-TUB1-URA3 KAN:pCUP:Arg:DHFR^{ts}:3HA:STU2*	This study
KBY2155	MATa *ndc10-2 his3-delta200 leu2-3, 112 ura3-52* Gal+ *ura3-52::GFP-TUBI-URA3* pAFS125	This study
KBY2161	MATa *ndc10-1 ura3 leu2 lys2 his3 trp1 ade2* pAFS125	This study
KBY2192	MATa *ctf13-30 ura3 lys2 ade2 his3 leu2* pAFS125	This study
KBY2154	MATa *ndc10-2 his3-delta200 leu2-3,112 ura3-52* Gal+ *trp::HYG cse4::KAN SPC29-CFP-NAT* pKK1	This study
KBY2165	MATa *ndc10-1 his3 leu2 ura3 lys2 trp1 ade2 cse4::HYG SPC29-CFP-KAN* pKK1	This study
KBY2666	MATa *ndc10-2 his3-delta200 leu2-3,112 ura3-52* Gal+ *ura3-52::GFP-TUB1-URA3* pAFS125 *KAN:pCUP:Arg:DHFR^{ts}:3HA:STU2*	This study
KBY2164	MATa *ndc10-1 ura3 leu2 lys2 his3 trp1 ade2* pAFS125 *KAN:pCUP:Arg:DHFR^{ts}:3HA:STU2*	This study
KBY2192	MATa *ctf13-30 ura3 lys2 ade2 his3 leu2* pAFS125 *KAN:pCUP:Arg:DHFR^{ts}:3HA:STU2*	This study

Plasmid name	Description/markers	Source/Reference
pCP21	CFP-NAT in pFA6	This study.
pBJ1212	pFA6a-KANMX6-pCUPts Degron-3HA	R. Heil-Chapdelaine
pDH3	CFP-KAN in pFA6	Yeast Resource Center
pAFS125	*ura3::TUB1-GFP-URA3*	Straight
pKK1	*CSE4-GFP* fusion, pRS314/*TRP1*	Keith/Baker/Fitzgerald-Hayes
pTub1GFP-Tub1	*TUB1-GFP-TUB1-TRP1*	Kosco/Huffaker

2000; Belmont, 2001; Pearson *et al*., 2001). Separated sister centromeres align into two clusters equidistant from the spindle equator (Pearson *et al*., 2001). Furthermore, centromeres oscillate along the spindle axis at rates similar to cytoplasmic microtubule plus-end dynamics (Pearson *et al*., 2001). Fluorescence redistribution after photobleaching (FRAP) studies have shown that microtubules turnover within the mitotic spindle. However, unlike tissue culture cells, turnover seems to be restricted to growth and shortening of kinetochore microtubule plus-ends (Maddox *et al*., 2000). Whether the kinetochore or microtubule binding proteins, or both, orchestrate chromosome dynamics can now be genetically dissected to identify the key regulatory pathways governing kinetochore microtubule dynamics and chromosome movement.

The primary candidate for regulating kinetochore microtubule dynamics is the conserved TOG/XMAP215/Dis1/Stu2p family of proteins. Stu2p localizes along the length of the mitotic spindle and is essential for anaphase spindle elongation, microtubule dynamics, and centromere positioning in *S. cerevisiae* (Kosco *et al*., 2001; Severin *et al*., 2001; He *et al*., 2001) and efficient chromosome segregation in *S. pombe* (Nabeshima *et al*., 1998). In vitro and in vivo, Stu2p binds to and selectively promotes dynamicity of microtubule plus-ends (Van Breugal *et al*., 2003). In the absence of Stu2p or XMAP215 (*Xenopus laevis*), microtubule plus-ends spend an increased time in a "paused" state identified by undetectable growth or shortening (Tran *et al*., 1997; Kosco *et al*., 2001; Shirasu-Hiza *et al*., 2003; Van Breugal *et al*., 2003). How Stu2p functions to create dynamic microtubule plus-ends is critical to understanding the overall mechanisms of chromosome motility.

We used live cell microscopy assays to dissect the role of Stu2p in regulating kinetochore microtubule dynamics and its effects on centromere motility and tension between sister centromeres. We found that Stu2p promotes dynamics at microtubule plus-ends, that maintaining kinetochore attachment and tension does not require dynamic microtubule plus-ends, and that kinetochores can promote microtubule dynamics independent of Stu2p.

MATERIALS AND METHODS

Plasmids

All plasmids are defined in Table 1. pCP21 (*CFP-NAT*) was generated by replacing the *Bgl*II/*Sac*I fragment containing KAN of pDH3 with the *Bgl*II/*Sac*I fragment containing natricin (NAT) from pAG31 (Dohmen *et al*., 1994). The *KAN:pCUP:Arg:DHFR^{ts}:3HA* (pBJ1212), CFP-KAN (pDH3), GFP-TUB1-URA3 (pAFS125), CSE4-GFP-TRP1 (pKK1), and TUB1-TUB1-GFP-TRP1 (pTub1-GFP-Tub1) plasmids were generous gifts from Dr. Richard Heil-Chapdelaine (Washington University, St. Louis, MO), Dr. Trisha Davis (Yeast Resource Center, University of Washington, Seattle, WA), Dr. Aaron Straight (Harvard University, Boston, MA) (Straight *et al*., 1997), Dr. Richard Baker (University of Massachusetts Medical School, Worcester, MA) (Chen *et al*., 2000), and Drs. Karena Kosco and Tim Huffaker (Cornell University, Ithaca, NY) (Kosco *et al*., 2001), respectively.

Polymerase Chain Reaction (PCR) Fragments for Integration

Fluorescently labeled spindle poles were constructed using primers to pFA6-GFP-KANMX6 plasmid flanked by 50 bp of homology one codon upstream of the stop codon and one codon downstream of the stop codon of the spindle

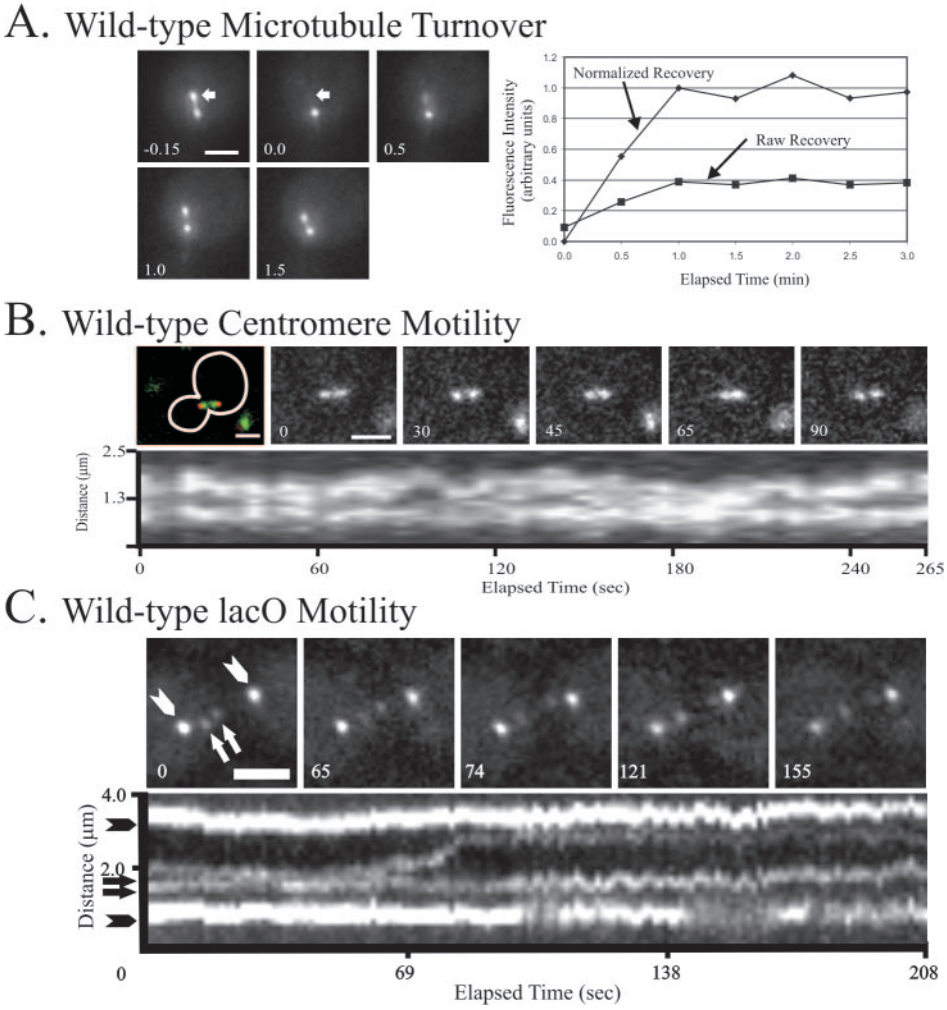

Figure 1. Microtubule turnover and centromere motility. (A) FRAP of wild-type mitotic spindles labeled with GFP-Tub1. The upper microtubule half-spindle (arrow) was photobleached by a short laser pulse (t = 0.0 min). Wild-type cells showed rapid, partial recovery ($t_{1/2}$ = 49 ± 18 s) of the bleached half-spindle. Normalized recovery is a ratio to equilibrate the percentage of recovery to the final wild-type fluorescence recovery. Time, min. (B) Centromeres, labeled with Cse4-GFP (green), and spindle poles labeled with Spc29-CFP (red) were imaged relative to each other in the first panel. The average distribution of spindle poles and centromeres was quantitated and summarized in Table 3. Cse4-GFP–labeled centromeres in the subsequent five panels and in the kymograph show single focal plane images acquired at 5-s intervals. Indicative of centromere motility, Cse4p localization in wild-type cells exhibited changes in the overall fluorescence distribution. Refer to Movie 1. (C) lacO chromosome marker ~1.1 kb from *CEN11* relative to Spc72-GFP–labeled spindle poles (Pearson *et al*., 2001). A single centromere proximal marker showed separation and movements relative to its sister centromere and spindle poles. Top, five selected frames of a time-lapse acquired at ~1-s intervals. Bottom, kymograph of the entire time-course. Spindle poles, arrowheads. lacO spots, arrows. Time, sec. Bar, 2 μm.

pole component *SPC29*. Integration sequences were amplified from either pCP21 (SPC29-CFP-NAT) or pDH3 (SPC29-CFP-KAN) (Yeast Resource Center).

Gene knockouts were performed using PCR-based deletions by amplifying heterologous drug-resistance marker cassettes flanked by 50 bp of homology to the gene being deleted (Wach *et al*., 1994; Longtine *et al*., 1998; Goldstein and McCusker, 1999). Deletions were confirmed by PCR amplification of flanking genomic DNA.

The *stu2* temperature degron system (*stu2^{td}*) was generated by PCR amplification of the *KAN:pCUP:Arg:DHFR^{ts}:3HA* cassette by using primers to the plasmid, pBJ1212, flanked by 50 bp of homology to the site of insertion at the start of *STU2*. pBJ1212 was adapted from a temperature-sensitive DHFR degron (Dohmen *et al*., 1994) with a copper-inducible promoter (Heil-Chapdelaine, unpublished data). The product was transformed to generate a strain with *KAN:pCUP:Arg:DHFR^{ts}:3HA* fused in frame to *STU2*. Proper integration and function was confirmed by PCR, temperature sensitivity, $CuSO_4$ sensitivity, and depletion of microtubule dynamics under repressing conditions similar to that previously shown for *stu2^{cu}* (Kosco *et al*., 2001).

Yeast Strains and Media

S. cerevisiae strains are listed in Table 1. Strains were maintained on YC complete media (0.67% yeast nitrogen base, 2% glucose, 0.5% casamino acids, with 0.05% adenine, 0.2% tryptophan, and 0.2% uracil). Experiments using copper-induced depletion of Stu2p cells (*stu2^{cu}*) were maintained on synthetic medium containing dextrose (0.67% yeast nitrogen base, 2% glucose, and the appropriate amino acids). To deplete cells of Stu2p, copper was added as described previously (Kosco *et al*., 2001). *stu2^{td}* cells were maintained in 100 μM $CuSO_4$ to maintain transcription of *stu2^{td}*. To deplete Stu2p, cells were shifted to 37°C without $CuSO_4$ for approximately 3 h. Conditional alleles of *ndc10* and *ctf13* were shifted to 37°C (from a 24°C permissive temperature) for approximately 3 h before imaging with a stage heater set to 35–39°C.

Drug Treatment

For azide treatment, midlogarithmic cells in YC complete media were washed with sterile water and incubated for 10 min on imaging slabs containing 0.02% azide (NaN_3; Sigma-Aldrich, St. Louis, MO) and 1.0 μM 2-deoxy-D-glucose as the only carbon source (Marshall *et al*., 1997).

For benomyl treatment, midlogarithmic cells in YC complete media were washed with sterile water and incubated for ~45 min on slabs containing ~15–30 μg/ml (35–50 μM) benomyl (DuPont, Wilmington, DE) in dimethyl sulfoxide (DMSO). The drug concentration was variable due to incomplete mixing of the benomyl solution with the slab media. We estimate that 35–50 μM is a higher concentration than the actual drug concentration in the cells.

For hydroxyurea (HU) experiments, midlogarithmic cells in YC complete media were treated with 200 mM HU for 1.5 h before shifting to 37°C for an additional 3 h before imaging.

Fluorescence Imaging

Techniques and equipment for fluorescent protein imaging have been described previously (Shaw *et al*., 1997; Maddox *et al*., 2000; Pearson *et al*., 2001). Static localization images were acquired in live cells by using 10 plane Z-series stacks at 0.5-μm steps. Fluorescence images with exposures of 250–750 ms were acquired for both green fluorescent protein (GFP) and cyan fluorescent protein (CFP). A single differential interference contrast image was acquired at the middle plane. Cse4-GFP centromere oscillations were observed by acquiring single GFP and CFP images at 5-s intervals. Epifluorescence acquisition settings and filter selection were described previously (Pearson *et al*., 2001). Centromere motility was judged based on the changes in distribution of Cse4-GFP. Changes in the compaction and fluorescence movements from the fluorescence cluster were interpreted to be centromere movements. Because spindle movement could contribute to the appearance of centromere movement, sequences where the spindle poles (labeled with CFP)

Table 2. Mitotic spindle fluorescence redistribution after photobleaching

Strain/Condition	Recovery half-time ($T_{1/2}$)	Normalized recovery[a]	No recovery[b]	P value	*n*
Wild type					
WT	49 ± 18	1.0 ± 0.3	0		7
WT (≈35–50 μM benomyl)	259 ± 130	0.6–1.0	0		5
WT (azide, deoxy-glucose)	N/A	N/A	5		5
Stu2p depletion					
WT (no $CuSO_4$)	40 ± 25	1.0 ± 0.2	0		3
Stu2p depleted (with $CuSO_4$)	233 ± 127	0.2 ± 0.0	2	0.035	4
stu2^{td} Permissive temperature	59 ± 31	1.0 ± 0.4	0		8
stu2^{td} Restrictive temperature	302 ± 200	0.9 ± 0.4	6	0.003[c]	21
Defective kinetochore (*ndc10-1*)					
ndc10-1 Permissive temperature	59 ± 20	1.0 ± 0.1	0		7
ndc10-1 Restrictive temperature	65 ± 29	1.2 ± 0.4	0	0.658[c]	6
Defective kinetochore (*ctf13-30*)					
ctf13-30 Permissive temperature	39 ± 15	1.0 ± 0.3	0		7
ctf13-30 Restrictive temperature	51 ± 21	1.2 ± 0.6	0	0.237[c]	8
Defective kinetochore (*ndc10-2*)					
ndc10-2 Permissive temperature	40 ± 14	1.0 ± 0.4	0		15
ndc10-2 Restrictive temperature bright	64 ± 42	1.0 ± 0.5	0	0.001[c]	13
ndc10-2 Restrictive temperature dim	60 ± 34	1.4 ± 0.5	0	0.001[c]	10
Stu2p depletion; Defective kinetochore					
stu2^{td}_ndc10-1 Permissive temperature	85 ± 44	1.0 ± 0.4	0	0.015[c]	10
stu2^{td}_ndc10-1 Restrictive temperature	205 ± 109	0.6 ± 0.3	10	0.159[d]	20
stu2^{td}_ctf13-30 Permissive temperature	72 ± 38	1.0 ± 0.3	0	<0.000[c]	10
stu2^{td}_ctf13-30 Restrictive temperature	330 ± 144	0.7 ± 0.3	4	0.730[c]	12
stu2^{td}_ndc10-2 Permissive temperature	124 ± 72	1.0 ± 0.4	1	0.085[c]	16
stu2^{td}_ndc10-2 Restrictive temperature	93 ± 46	0.9 ± 0.4	3	<0.000[d]	35

[a] Normalized recovery is the fraction of the final percentage of recovery compared to wild-type or permissive conditions (MATERIALS AND METHODS).

[b] No measurable recovery of fluorescence intensity was observed in these cells.

[c] P value ($t_{1/2}$) compared with permissive conditions.

[d] P value ($t_{1/2}$) compared with *stu2^{td}* alone at restrictive condition.

rotated out of the focal plane for greater than 15 s were not analyzed. Qualitative measurements of centromere movement were defined for each condition as ++ (wild-type motility), +− (decreased motility), and − (no observable movement). Each time lapse is representative of at least five individual time lapses.

Centromere proximal lac operator (lacO) movements were followed relative to GFP-labeled spindle poles at ~1-s intervals as described previously (Pearson *et al.*, 2001). Centromere motility with a single lacO marker was judged by observation of "directed movements." A directed movement was defined as a movement in a continuous direction in five consecutive frames (Pearson *et al.*, 2001). Each time-lapse is representative of at least five time-lapse sequences.

Fluorescence Recovery after Photobleaching

The techniques and equipment used for FRAP were described previously (Maddox *et al.*, 2000). Cells containing GFP-TUB1 were treated with a 35-ms, 488-nm laser exposure focused to one-half of the mitotic spindle. Bleached spindles were then monitored for fluorescence recovery at 30-s, 1-min, or 2-min intervals by using a five plane optical Z-series acquisition. Images were then compiled to a single plane maximum projection that was quantitated as described by Maddox *et al.* (2000). Loss of fluorescence was also observed in the opposing unbleached half-spindle (data not shown), indicating that bleached GFP-Tub1 exchanged into the unbleached half-spindle with similar kinetics. Partial recovery of the half-spindle is due to the stable interpolar microtubules that do not recover and the limited pool of GFP-Tub1 (Maddox *et al.*, 2000). For each sequence, the half-time to recovery ($t_{1/2}$) and normalized recovery of the bleach pole was calculated. The normalized recovery was calculated as the fraction of the final fluorescence recovery relative to wild-type or permissive conditions (normalized recovery = $F_{\text{final fluorescence}}/F_{\text{wild-type final fluorescence}}$). No recovery was determined for cells showing 5% (16% normalized recovery) or less at the final time point (these data were not included in the recovery statistics).

Spindle Structure Measurements

The distance measurements for spindle length, centromere separation, and metaphase localization were all measured and calculated as described previously (Pearson *et al.*, 2001). Briefly, stacks were analyzed in three dimensions to determine the localization of spindle poles and centromere clusters relative to each other. The data were exported to an Excel spreadsheet for further analyses (Excel; Microsoft, Redmond, WA).

Image Presentation

Images and kymographs were prepared using both MetaMorph Imaging software (Universal Imaging, Downingtown, PA) and Corel 11 (Corel, Ottawa, Ontario, Canada).

RESULTS

Spindle Microtubule Turnover Is Essential for Centromere Motility but Not Separation

To investigate the role of microtubule dynamics in metaphase sister centromere separation and motility, we observed centromeres when microtubules were experimentally stabilized. Microtubule dynamics in tissue cells is suppressed in vitro and in vivo by substoichiometric concentrations of the microtubule-destabilizing drugs vinblastine and nocadozole (Toso *et al.*, 1993; Dhamodharan *et al.*, 1995; Vasquez *et al.*, 1997). To suppress microtubule dynamics in budding yeast, cells expressing green fluorescent protein (GFP)-Tub1 were treated with low concentrations of a similar drug, benomyl, and spindle microtubule turnover was assayed by FRAP. In wild-type cells, the half-spindle recovers 35 ± 11% with a $t_{1/2}$ of 49 ± 18 s (Figure 1A and Table 2) (Maddox *et al.*, 2000). The incomplete recovery is likely due to the stable class of interpolar microtubules and the limited free pool of unbleached GFP-tubulin (Maddox *et al.*,

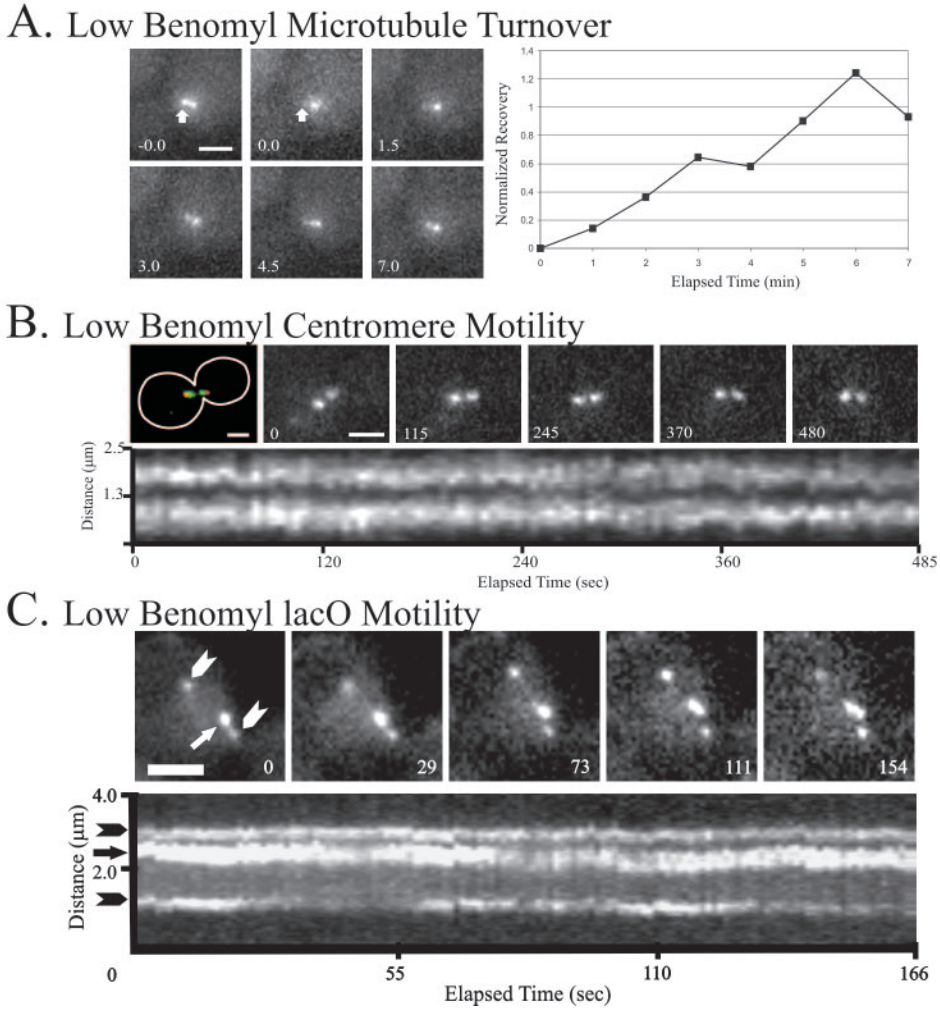

Figure 2. Decreased microtubule turnover and centromere motility in low concentrations of benomyl. (A) The rate of GFP-Tub1 FRAP was decreased in low concentrations of benomyl. Microtubule tufts were still evident, indicating that the decreased turnover was not due to loss of microtubule polymer. (B) Cells treated with low concentrations of benomyl exhibited decreased centromere motility but maintained metaphase alignment. The first panel shows normal metaphase alignment. The following frames and kymograph describe severely decreased centromere motility. Refer to Movie 2. (C) Centromere proximal lacO markers in cells treated with low concentrations of benomyl showed decreased separation and frequency of oscillations. lacO markers did not oscillate relative to spindle poles. Spindle poles, arrowheads. lacO spots, arrows. Time, sec. Bar, 2 μm.

2000). For comparison of the percentage of recovery, FRAP measurements were normalized to the average wild-type fluorescence recovery to produce "normalized FRAP" measurements (Figure 1A and Table 2). In cells treated with low benomyl concentrations, spindle structure, and kinetochore-microtubule attachment was maintained; however, the rate of fluorescence recovery decreased fivefold (259 ± 130 s). The final recovery of the bleached half-spindle was less than wild-

Table 3. Mitotic centromere localization and spindle length

Strain/Condition description	Centromere separation[a] μm	Spindle length μm	Metaphase cells %	n
WT (Cse4-GFP, Spc29-CFP)				
WT	0.9 ± 0.3	1.7 ± 0.3	98	101
WT (≈35–50 μM benomyl)	0.7 ± 0.4	1.4 ± 0.4	90	101
WT (azide, deoxy-glucose)	0.7 ± 0.2	1.5 ± 0.3	94	93
stu2^{td} depletion(Cse4-GFP, Spc29-CFP)				
WT (no $CuSO_4$)	0.9 ± 0.3	1.6 ± 0.3	90	100
Stu2p depleted (with $CuSO_4$)	0.4 ± 0.4	1.6 ± 0.4	84	69
ndc10-2 (Cse4-GFP, Spc29-CFP)				
Permissive temperature	0.6 ± 0.4	1.4 ± 0.4	N/A	42
Restrictive temperature	N/A[b]	2.9 ± 0.9	N/A	43

[a] Centroid to centroid distance of clustered centromeres.

[b] The average centromere cluster length was not determined because Cse4-GFP signal was not detected.

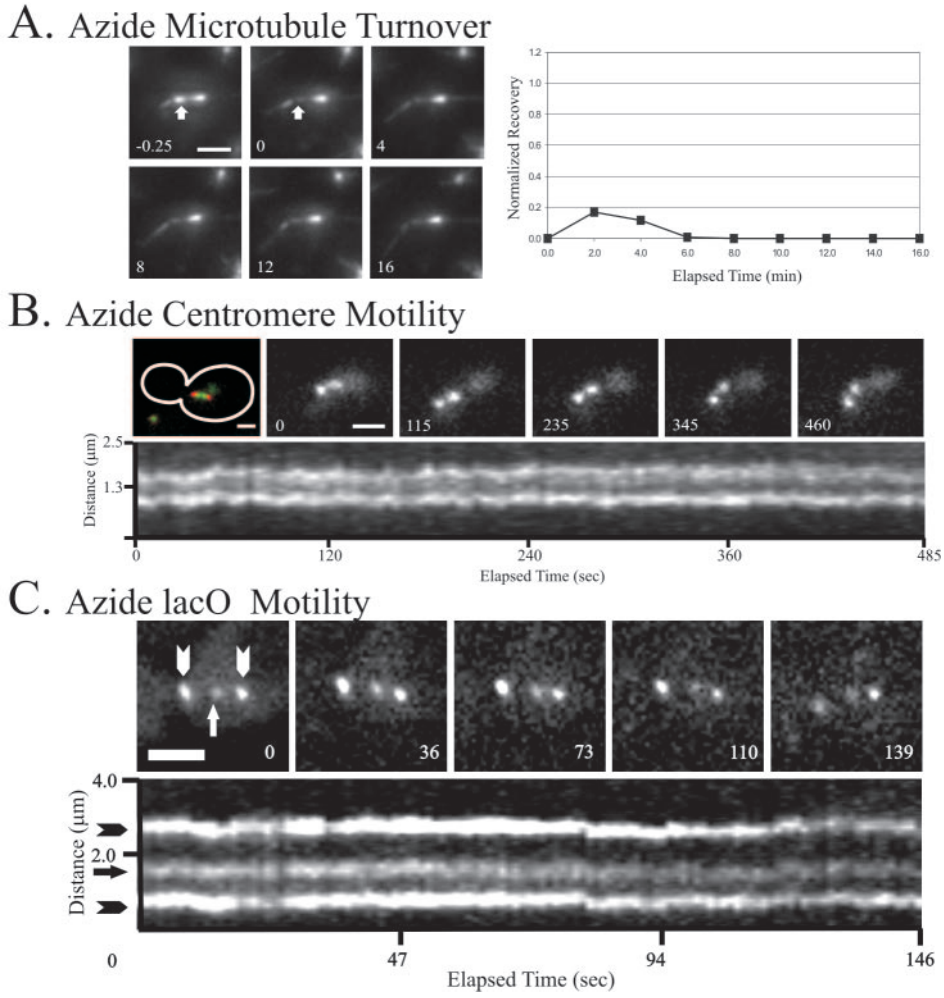

Figure 3. Decreased microtubule turnover and centromere motility in azide-treated cells. (A) FRAP of GFP-Tub1p was severely retarded in cells treated with metabolic inhibitors. This is observed by the lack of fluorescence recovery in the bleached half-spindle. However, microtubule tufts are still evident, indicating that the overall structure of the spindle is maintained. (B) Centromere localization relative to spindle poles displays normal kinetochore attachment, sister separation, and spindle structure (first panel). Subsequent panels and kymograph show decreased changes in fluorescence distribution compared with wild type. Thus, reduced centromere motility occurs in cells treated with metabolic inhibitors. Refer to Movie 3. (C) Centromere proximal lacO markers were not as separated as wild-type and did not oscillate along the length of the spindle. Spindle poles, arrowheads. lacO spots, arrows. Time, sec. Bar, 2 μm.

type levels (normalized recovery, 0.6–1.0; Figures 2A and 5 and Table 2). These data indicate that, similar to vinblastine- and nocodazole-treated tissue cells, spindle microtubules in *S. cerevisiae* are stabilized by low concentrations of benomyl.

To determine whether microtubule dynamics contributed to tension on sister chromatids, we measured the metaphase position of the centromere-specific histone protein Cse4-GFP, relative to spindle poles labeled with Spc29-CFP. The average separation of sister centromere clusters in large budded wild-type cells before anaphase was 0.9 $\pm$ 0.3 μm with an average spindle length of 1.7 $\pm$ 0.3 μm (Table 3 and Figure 1B). In cells treated with low concentrations of benomyl, sister centromeres remained separated into two clusters, but the average separation (0.7 $\pm$ 0.4 μm), spindle length (1.4 $\pm$ 0.4 μm), and percentage of population at metaphase (90%) were all decreased. In low benomyl concentrations, the overall spindle structure remained intact (Table 3 and Figure 2B). The decrease in separation of sister centromeres in individual cells was proportional to the decrease in spindle length. Thus, the average length of kinetochore microtubules did not change as drastically as spindle length (our unpublished data).

Centromere oscillations were examined using either GFP-labeled kinetochores (Cse4-GFP; Figure 1B) or a centromere proximal lacO marker relative to fluorescently labeled spindle poles. Centromere oscillations were determined by changes in the width and distribution of Cse4-GFP clusters along the length of the spindle axis. Consistent with the decrease in microtubule dynamics (Figure 2A), centromere oscillations were reduced in the presence of benomyl, whereas kinetochore microtubule attachment remained intact (Figure 2B). Figure 2B shows normal sister centromere separation and clustering, indicating that there was no loss in kinetochore attachment. However, compared with wild type (Figure 1B), centromere oscillations were decreased as indicated by the narrow clusters and decreased fluorescence between the clusters (Figure 2B). Oscillations of a single centromere pair observed by lacO spot movements relative to each other and to GFP-labeled spindle poles (Figure 1C) were decreased in cells treated with low concentrations of benomyl (Figure 2C).

Metabolic inhibitors provide an alternative method to inhibit spindle microtubule turnover in tissue cells (Wadsworth and Salmon, 1988). Azide and deoxy-glucose also inhibit microtubule turnover and centromere movements in yeast. No substantial half-spindle turnover (<16% normalized recovery) was observed in drug-treated cells after photobleaching (Figures 3A and 5 and Table 2). Thus, cells require ATP for growth and shortening of spindle microtubules. The spindle structure in azide-treated cells was similar to wild type (Figure 3B, first panel). The average separation of sister centromeres was 0.7 $\pm$ 0.2 μm with a spindle

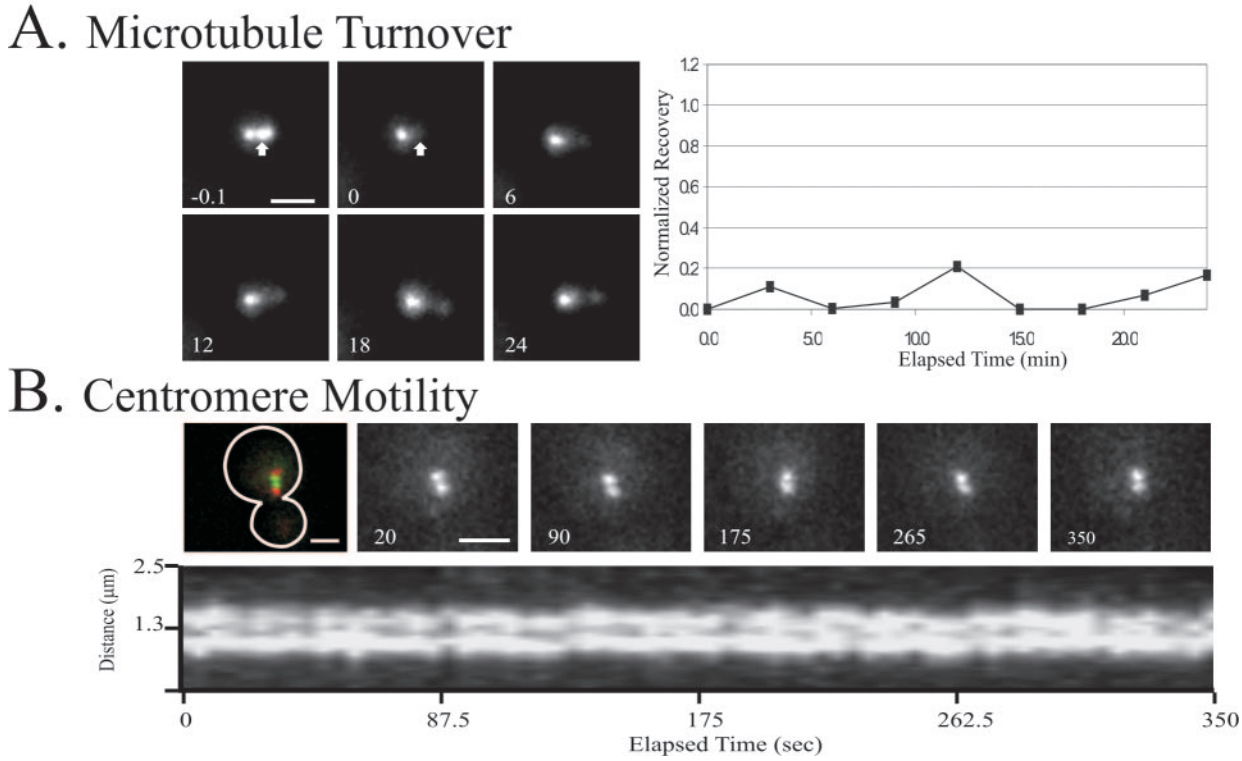

Figure 4. Stu2p is essential for promoting spindle microtubule dynamics. (A) Cells depleted of Stu2p (*stu2*^{cu}) showed severely decreased microtubule turnover. In this example, the bleached half-spindle showed very low recovery after 24 min. Similar results were also found for the *stu2*^{td} system (Figure 9) Time, min. (B) Cells (stu2^{cu}) treated with copper showed decreased centromere motility (panels and kymograph), while maintaining sister separation and metaphase alignment. Refer to Movie 4. Time, sec. Bar, 2 μm.

length of 1.5 ± 0.3 μm (Table 3). Large budded cells showed metaphase alignment in 94% of the cells indicating that most cells maintained metaphase spindle organization in the absence of microtubule dynamics (Table 3). Furthermore, centromere oscillations were inhibited by ATP depletion (Figure 3, B and C). Sister centromere markers were less separated (Figure 3C) compared with wild-type conditions (Figure 1C), likely due to a decrease in spindle length.

Importantly, loss of microtubule turnover inhibits centromere motility without breaking kinetochore-microtubule attachment. Thus, microtubule dynamics is coupled to centromere oscillations. Once sister centromeres are separated, maintenance of kinetochore tension does not require kinetochore microtubule dynamics or ATP.

Reduced Spindle Microtubule Turnover and Centromere Motility in the Absence of Stu2p

To understand the regulatory mechanisms for microtubule dynamics and centromere movements, we used genetic mutations that affect spindle microtubule turnover. Depletion of Stu2p (*stu2*^{cu}) severely decreases microtubule turnover (Kosco *et al*., 2001). The rate ($t_{1/2}$) was approximately sixfold slower (233 ± 127 s) compared with wild type with a low normalized recovery (0.2 ± 0.0; Figures 4A and 5 and Table 2) (Kosco *et al*., 2001). Two of four cells exhibited no measurable recovery after 20 min. To create a rapid Stu2p protein degradation system that could be easily moved to different strain backgrounds, we used a heat inducible degron (*stu2*^{td}) under the control of a conditional transcriptional promoter (Dohmen *et al*., 1994; Heil-Chapdelaine; unpublished data). Stu2p depletion by using the degron (*stu2*^{td}) was similar to the *stu2*^{cu} system. The rate of spindle microtubule turnover decreased sixfold (302 ± 200 s) compared with permissive conditions (59 ± 31 s; Figures 4A and 5 and Table 2). The normalized final recovery was greater than *stu2*^{cu} mutants (0.9 ± 0.4; Figures 4A and 5 and Table 2). This may be due to incomplete depletion of Stu2p. Six of 21 cells exhibited no measurable recovery (Table 2). Therefore, Stu2p promotes kinetochore microtubule turnover (Kosco *et al*., 2001) by relieving the paused state observed in the absence of Stu2p (Kosco *et al*., 2001; Shirasu-Hiza *et al*., 2003; Van Breugal *et al*., 2003).

The photobleaching experiments do not distinguish between defects in nucleation of new kinetochore microtubules and persistent attachment of existing kinetochore microtubules. To distinguish between these possibilities, we examined whether centromeres collapsed (loss of kinetochore microtubules) or remained separated (persistent attachment) after depletion of Stu2p. The overall centromere separation (Cse4-GFP) and spindle structure was maintained in cells lacking Stu2p. The distance between separated centromeres was decreased (0.4 ± 0.4 μm), and the spindle length unchanged (1.6 ± 0.4 μm; Table 3), relative to wild type (0.9 ± 0.3 μm and 1.6 ± 0.3 μm, respectively). The large SD in average separation is consistent with the range of centromere distributions observed in Stu2p-depleted cells (Kosco *et al*., 2001). Greater than 40% of the Stu2p depleted cells have a single Cse4-GFP cluster compared with 0% for wild-type cells (our

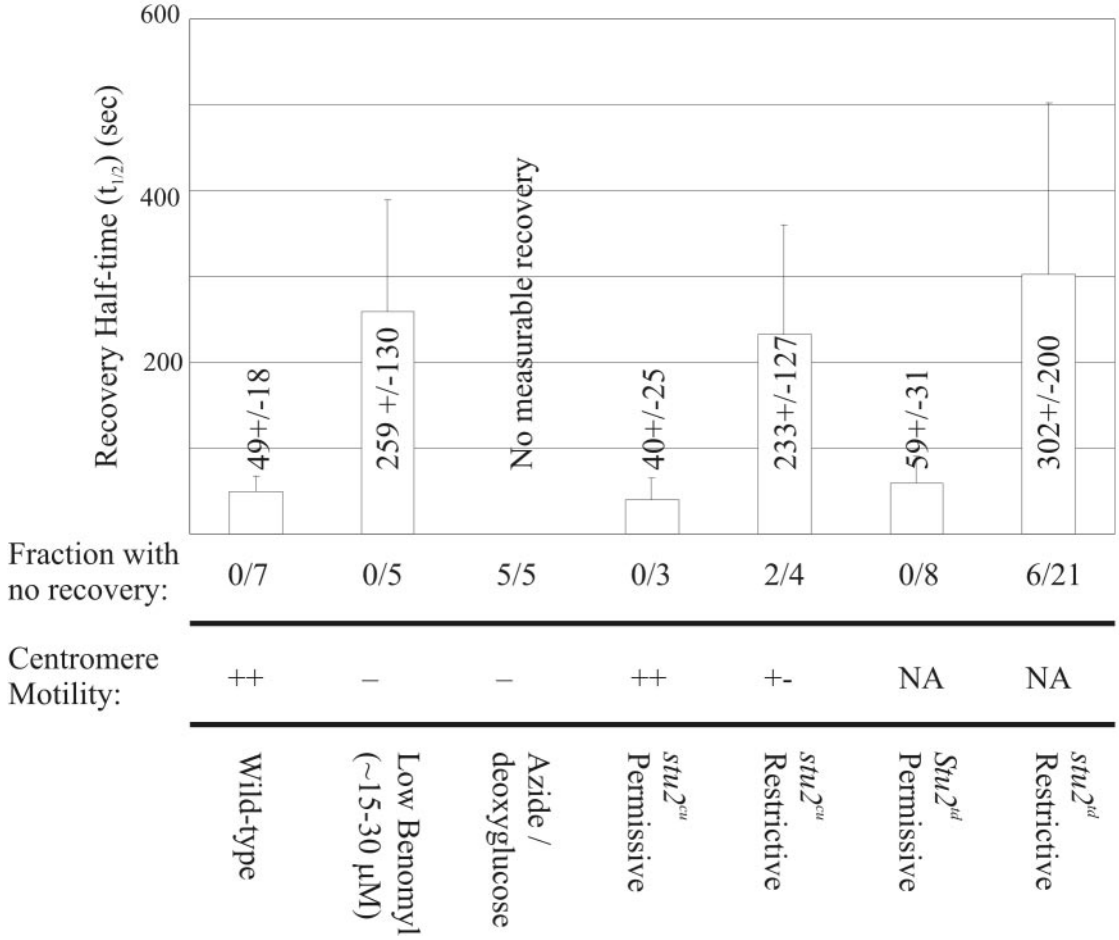

Figure 5. Spindle microtubule dynamics driven by Stu2p are necessary for centromere motility. Comparison of $t_{1/2}$ of bleached spindle microtubules for wild-type, azide/deoxy-glucose, low benomyl, *stu2*^{cu} and *stu2*^{td}. The experiments without recovery (normalized recovery <16%) were not included in the recovery measurements. Qualitative analysis of centromere motility is presented for comparison with the microtubule turnover.

unpublished data). Depletion of Stu2p requires approximately 2 h, whereas azide and benomyl act within minutes (Kosco *et al.*, 2001). The relatively slow depletion time may result in a mixed population; one that has entered mitosis, but is unable to generate either bipolar attachments and/or force to produce tension, another in which separated centromeres are maintained even after Stu2p depletion. Metaphase alignment was observed in 84% of the cells (Table 3). Centromere oscillations were diminished in metaphase, indicative of decreased microtubule dynamics upon Stu2p depletion (Figure 4B). Thus, kinetochore microtubules persist in the paused state in the absence of Stu2p and centromere separation does not require dynamic microtubule plus-ends.

Disruption of Kinetochore Function Does Not Severely Alter Microtubule Dynamics

The stabilization of microtubules bound to kinetochores in tissue cells indicates there is a kinetochore-dependent regulation of microtubule dynamics (Mitchison *et al.*, 1986; Zhai *et al.*, 1995; Hunt and McIntosh, 1998). To determine whether the kinetochore itself promotes microtubule dynamics, microtubule turnover was measured in core kinetochore mutants (*NDC10* and *CTF13*) that fail to generate proper kinetochore-microtubule attachments (Doheny *et al.*, 1993; Goh and Kilmartin, 1993; Jiang *et al.*, 1993; Hyman and Sorger, 1995; Kopski and Huffaker, 1997).

The *ndc10-1* mutant at restrictive temperature displayed variably longer, asymmetric spindles with turnover rates (65 ± 29 s) indistinguishable from permissive temperature (59 ± 20 s; p = 0.658; Table 2). Normalized recovery was increased compared with permissive conditions (1.2 ± 0.4; Table 2). *ctf13-30* mutants displayed normal spindle lengths without asymmetric half-spindles at restrictive temperature (our unpublished data). Microtubule turnover rates in *ctf13-30* (51 ± 21 s) were not significantly different from permissive temperature (39 ± 15 s; p = 0.237) (Table 2). Similar to *ndc10-1*, *ctf13-30* cells at restrictive temperature had a slight but measurable increased recovery compared with permissive conditions (1.2 ± 0.6; Table 2). *ndc10-2* spindles were longer and asymmetric at restrictive temperature compared with permissive conditions (Table 3). Asymmetric distributions of GFP-Tub1 fluorescence with one bright half-spindle and an opposing half-spindle with decreased fluorescence intensity were observed in ~45% of large budded cells (Table 3 and Figure 6; our unpublished

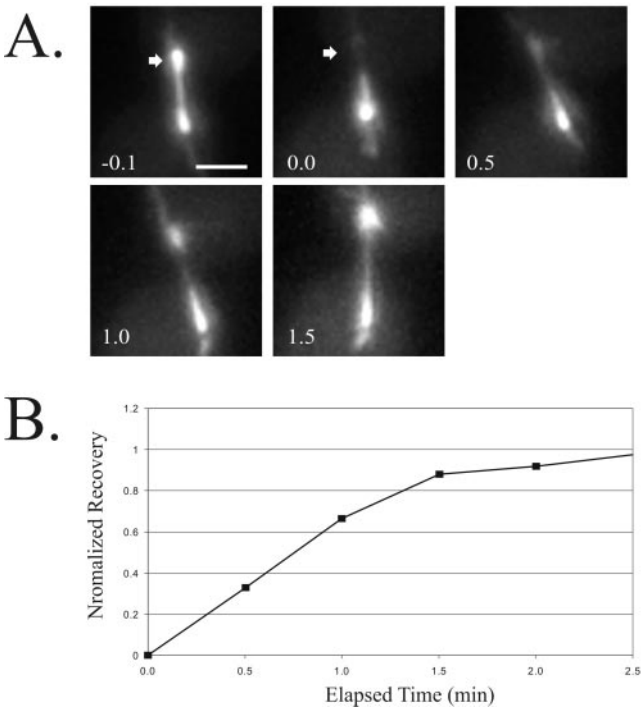

Figure 6. Mutations in kinetochore function do not severely affect spindle microtubule dynamics. GFP-Tub1 turnover in mitotic spindles was measured in *ndc10-1*, *ctf13-30*, and *ndc10-2* cells at restrictive temperature. The overall spindle length was longer and approximately one-half of the cell population showed an asymmetric microtubule distribution with one microtubule tuft or half-spindle brighter than the other. Figure describes a representative example of FRAP of kinetochore mutants (example was *ndc10-2*). The average turnover rate was slightly decreased compared with permissive conditions (64 ± 42 s [bright] and 60 ± 34 s [dim] vs. 40 ± 14 s). Similar results were found for *ndc10-1* and *ctf13-30* mutants (Table 2) however *ctf13-30* did not display longer, asymmetric spindles. Time, min. Bar, 2 μm.

data). The turnover of both halves of asymmetric spindles for *ndc10-2* cells at restrictive temperature was measured. Each class of half-spindle recovered similarly ($p = 0.955$) with a $t_{1/2}$ of 64 ± 42 s and 60 ± 34 s, respectively (Figure 6 and Table 2), slightly slower than permissive temperature (40 ± 14 s; $p = 0.001$ and 0.001, respectively). The normalized recovery was 1.0 ± 0.5 and 1.4 ± 0.5, respectively (Table 2). Although the differences between permissive and restrictive conditions were not statistically significant for *ndc10-1* or *ctf13-30*, the CBF3 components showed a reproducible decrease in the rate of recovery. *ndc10-2* cells displayed the only statistically significant change in the rate of recovery compared with permissive conditions.

The difference in tubulin turnover of each kinetochore mutation is indicative of differential functional effects on the kinetochore leading to altered regulation of microtubule dynamics. To assay the severity of each kinetochore mutant allele on kinetochore function, we measured the localization of Cse4-GFP in cells that achieved a bipolar attachment by arrest in hydroxyurea. Hydroxyurea arrests the cell cycle with bioriented attachment of sister kinetochores to each spindle pole (Goshima and Yanagida, 2000). Spindles in *ndc10-1* mutants arrested in hydroxyurea before temperature shift showed longer spindles (3.1 ± 0.7 μm) and punctate Cse4-GFP localization in only 10% of the cells (Figure 7). The remaining cells had a diffuse Cse4-GFP signal throughout the nucleus. In contrast, spindles in *ndc10-2* mutants shifted to restrictive temperature after hydroxyurea arrest maintained a normal metaphase length of 1.5 ± 0.5 μm and distinct Cse4-GFP localization at the kinetochore in 97% of the population. However, metaphase alignment was aberrant in many cells (69%) with centromeres localized as a single cluster or along the spindle axis (Figure 7). These results indicate *ndc10-1* severely disrupts the kinetochore as previously described (Doheny *et al*., 1993; Goh and Kilmartin, 1993). *ndc10-2* generates partially functional kinetochores unable to efficiently congress or separate sister centromeres during metaphase (Figure 7). To determine the molecular difference between the *ndc10* alleles, the *ndc10* alleles in each strain were sequenced and compared with wild type. *ndc10-1* contains an ochre mutation (Q944*) generating a carboxy terminal truncation of 12 amino acids; *ndc10-2* contains a single transition mutation (A914T) in the carboxy terminus.

These data indicate proper kinetochore function is not essential for promoting dynamic spindle microtubules. Loss of kinetochore structure and microtubule attachment (*ndc10-1*) did not severely affect spindle microtubule dynamics or turnover. However, a partial mutant (*ndc10-2*) produces a measurable decrease in the rate of spindle microtubule turnover. Therefore, alterations in kinetochore function indeed influence spindle microtubule dynamics.

Kinetochore Regulation of Microtubule Dynamics in the Absence of Stu2p

The decreased microtubule turnover in the absence of Stu2p provides the opportunity to determine kinetochore specific contributions to generating dynamic microtubules. To dissect the role of kinetochores in regulating microtubule dynamics, we depleted Stu2p (*stu2^{td}*) in each of the previously studied CBF3 mutants (*ndc10-1*, *ctf13-30*, and *ndc10-2*).

The rate of spindle microtubule recovery did not increase in the *stu2^{td}*, *ndc10-1*, or *stu2^{td}*, *ctf13-30* double mutants. *stu2^{td}*, *ndc10-1* at restrictive temperature had an average recovery rate of 205 ± 109 s compared with 85 ± 44 s for permissive temperature ($p = 0.015$; Figure 8). Half of the cells showed no fluorescence recovery (Table 2). The rate of turnover was not significantly different from *stu2^{td}* alone at restrictive temperature ($p = 0.159$; Table 2). *stu2^{td}*, *ctf13-30* cells exhibited an average recovery half-time of 330 ± 144 s at restrictive temperature and 72 ± 38 s at permissive temperature. No significant difference was observed between *stu2^{td}* and *stu2^{td}*, *ctf13-30* at restrictive temperature ($p = 0.730$). No recovery was observed in four cells at restrictive temperature (Table 2). Thus, mutations that completely disrupt kinetochore organization do not affect microtubule turnover (Figure 9). Stabilization of microtubules in the absence of Stu2p is therefore independent of kinetochore attachment.

To determine whether partially functional kinetochores (*ndc10-2*) affect the stable microtubule population in *stu2^{td}*, photobleaching was performed in *stu2^{td}*, *ndc10-2* cells. At permissive temperature, *stu2^{td}*, *ndc10-2* double mutants showed a slower recovery compared with wild-type cells (124 ± 72 s; Figures 8 and 9). Cells shifted to restrictive temperature showed an increased rate of microtubule turnover (93 ± 46 s; Figures 8 and 9). Three of 21 cells exhibited no recovery. This recovery was significantly faster than *stu2^{td}* alone ($t_{1/2} = 302 \pm 200$ s; $p < 0.000$). Thus, analysis of microtubule dynamics in *ndc10-2* revealed that kinetochores have the capacity to regulate kinetochore microtubule dynamics.

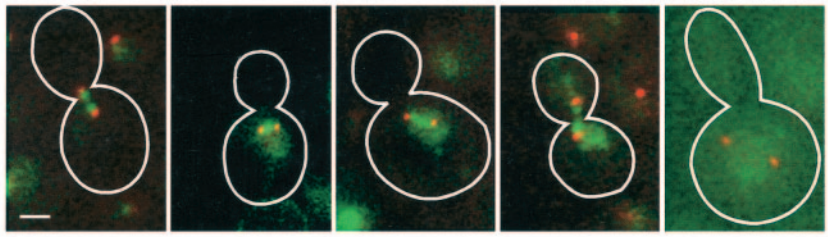

Strain	Ave spindle length	Metaphase	Single Focused Cluster	Elongated Cluster	Uneven Distribution	No Cse4-GFP Localization	Total Cells
	μm	%	%	%	%	%	n
WT Permissive temp.	2.0±0.5	77	8	11	0	4	53
ndc10-1 Restrictive temp.	N/A[a]	0	10	4	0	86	77
HU treated *ndc10-1*	3.1±0.7	0	5	5	0	90	110
WT Permissive temp.	1.4±0.4	70	6	18	8	0	40
ndc10-2 Restrictive temp.	2.8±0.9	16	0	7	16	60	43
HU treated *ndc10-2*	1.2±0.5	29	29	40	0	3	44

[a] Asynchronous *ndc10-1* cells shifted to restrictive for 3 h do not show Cse4-GFP or Spc29-CFP spindle pole signal and therefore spindle length could not be measured. Because hydroxyurea (HU) treated cells do not show a loss in Spc29-CFP signal the loss in signal in asynchronous cells is likely due to loss in Ndc10p function.

Figure 7. Kinetochore function in *ndc10-1* and *ndc10-2* mutants. *ndc10-1* showed increased kinetochore disruption compared with *ndc10-2* mutants. *ndc10-1* spindles arrested with a bipolar attachment in hydroxyurea before shifting to restrictive temperature showed no Cse4-GFP–labeled spindle poles. *ndc10-1* spindles were much longer than wild-type metaphase spindles. In contrast, *ndc10-2* spindles arrested in a bipolar attachment before temperature shift showed Cse4-GFP signal in 97% of cells analyzed. However, metaphase alignment was severely decreased. These results indicated that the *ndc10-1* mutation may completely disrupt the kinetochore in metaphase, whereas *ndc10-2* generated a partial kinetochore mutation that cannot efficiently congress to metaphase. Bar, 2 μm.

DISCUSSION

During mitosis, spindle microtubule plus-ends undergo a transition in their microenvironment. Free from kinetochore association, dynamic microtubules search the nucleoplasm to gain proper bipolar attachment to the kinetochore. On attachment, microtubule plus-ends interact with kinetochores producing force required for centromere oscillations and congression to the metaphase plate. Microtubules persist at kinetochores in a paused state in *stu2* mutants, indicating that Stu2p promotes microtubule plus-end dynamics. Once sister centromere separation is established, tension between sister chromatids can be maintained in the absence of normal microtubule dynamics. Although the kinetochore is dispensable for microtubule dynamics, specific mutant alleles (*ndc10-2*) promote dynamics of paused microtubules. Thus, Ndc10p and therefore the kinetochore can regulate microtubule dynamics.

Spindle Microtubule Dynamics Is Needed for Centromere Motility but Not Tension between Sister Centromeres

The movement of centromeres between spindle poles before and during metaphase requires dynamic microtubules. Inhibition of spindle microtubule dynamics coincides with a reduction in centromere oscillations. Interestingly, centromere distribution and tension were relatively unaffected by decreased microtubule dynamics. Maintenance of attachment and tension between sister chromatids, but not centromere oscillations, can occur with severely reduced kinetochore microtubule growth and shortening. Thus, dynamic microtubules are required to generate force for sister centromere separation and congression to the metaphase plate, but not for maintaining tension or metaphase (Figure 10C).

Experiments in tissue cells show that kinetochore-microtubule attachment is maintained in low concentrations of vinblastine; however, unlike budding yeast, tension between sister centromeres (measured by their separation) is severely reduced (44%) (Skoufias *et al.*, 2001). The dissimilarity likely reflects the large difference in spindle dimensions in yeast compared with tissue cells. If the stabilized kinetochore microtubule length remains constant, a short decrease in spindle length causes a large change in centromere separation in tissue cells. Conversely, a small decrease in spindle length in budding yeast coincides with more subtle effects on centromere separation. The maintenance of tension in the absence of microtubule dynamics is likely a conserved feature of eukaryotic kinetochores.

Stu2p Promotes Spindle Microtubule Dynamics

Kinetochore microtubule turnover as well as centromere motility was decreased in Stu2p-depleted cells (Figure 4A) (Kosco *et al.*, 2001; He *et al.*, 2001). Thus, Stu2p promotes kinetochore microtubule dynamics and centromere movements in vivo but is not required to maintain kinetochore

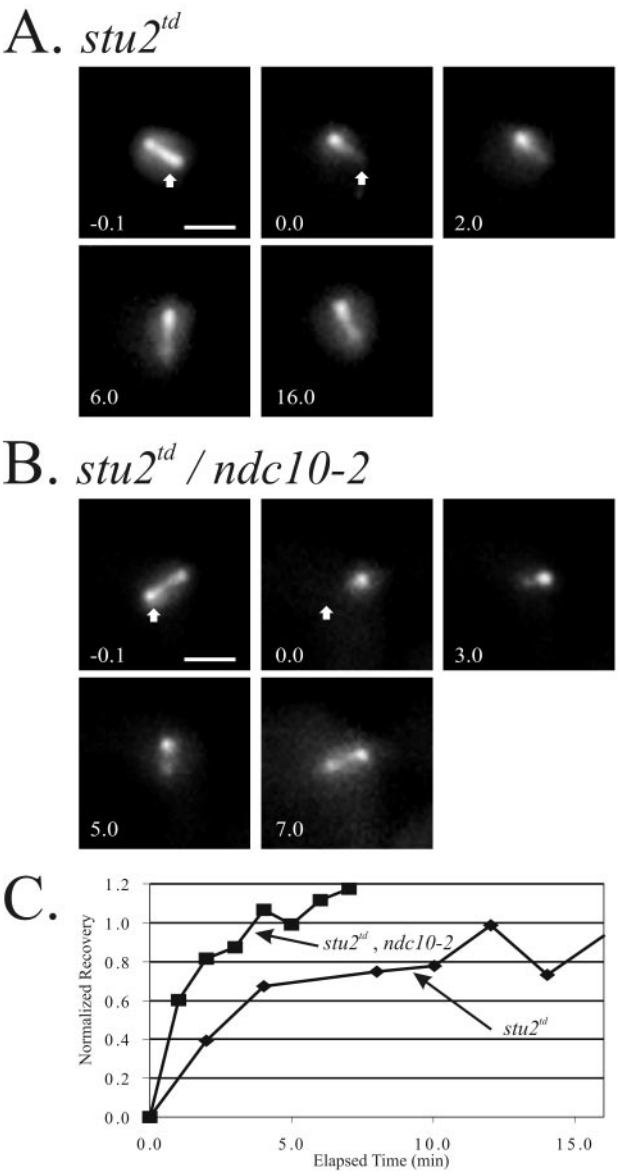

Figure 8. *ndc10-2* kinetochore allele rescues spindle microtubule turnover in *stu2*^{td} mutants. (A) FRAP of GFP-Tub1–labeled mitotic half-spindles in Stu2p depleted cells. Representative sequence and fluorescence intensity measurements showed slowed ($t_{1/2}$ = 302 ± 200 s) and slightly decreased spindle microtubule turnover (normalized recovery = 0.9 ± 0.4). (B) Microtubule turnover in *stu2*^{td} and *ndc10-2* double mutants increased the turnover rate ($t_{1/2}$ = 93 ± 46 s) with a similar normalized recovery compared with *stu2*^{td} alone (0.9 ± 0.4). (C) Example recovery curves of *stu2*^{td} alone and *stu2*^{td}, *ndc10-2* double mutants. Time, min. Bar, 2 μm.

attachment to microtubules or sister centromere tension (Figure 10C). Therefore, Stu2p's role is not in attachment; rather, it is in the transition from the paused state facilitating microtubule shortening and/or growth (Figure 10C). Stu2p increases catastrophe events during growth and rescue events during shortening (Kosco *et al*., 2001). Stu2p likely functions together with other microtubule binding proteins to increase microtubule transition frequencies by the recruitment of growth factors to shortening ends and catastrophe factors to growing ends (Kinoshita *et al*., 2001, 2002; Andersen and Wittmann, 2002). The dynamic microtubule state is necessary to gain proper centromere attachment and positioning, Stu2p promotes this by preventing prolonged pauses of microtubule plus-ends (Kosco *et al*., 2001; Shirasu-Hiza *et al*., 2003; Van Breugal *et al*., 2003).

Stu2p Promotes Spindle Microtubule Dynamics Independent of the Kinetochore

Stu2p's localization to the kinetochore (Kosco *et al*., 2001; He *et al*., 2001) suggests the kinetochore may contribute to Stu2p's ability to promote spindle microtubule dynamics. We measured microtubule turnover in cells with aberrant kinetochores (*ndc10-1*, *ctf13-30*, and *ndc10-2*). Nonfunctional kinetochores (*ndc10-1*) did not substantially affect the rate of kinetochore microtubule turnover. Therefore, the interaction of microtubules with kinetochores is not essential for Stu2p to promote microtubule dynamics (Figure 10B). A functional distinction between *ndc10-1* and *ndc10-2* was observed in the rates of microtubule turnover. The decreased turnover rate in *ndc10-2* mutants may reflect kinetochore-dependent changes in microtubule dynamics. Thus, kinetochore disruption did not lead to stabilization of microtubules, as we observed for *stu2* mutants; however, small changes in turnover occur in *ndc10-2* mutants. These data extend studies on Stu2p's role in promoting cytoplasmic microtubule dynamics.

Three possible models for rapid recovery of spindle microtubules are kinetochore microtubule plus-end growth and shortening, translocation of the microtubule lattice to the spindle pole or poleward microtubule flux, and continual detachment and reattachment of microtubules to kinetochores. Several lines of evidence suggest that Stu2p is responsible for promoting kinetochore microtubule plus-end dynamics that enables GFP-Tub1 turnover in the mitotic spindle. Electron microscopy studies show yeast kinetochore microtubule plus-ends exhibit open, "peeling or rams horn" structure indicative of shortening microtubules, whereas minus-ends at the spindle pole display a closed, tapered structure consistent with stable microtubules (Byers *et al*., 1978; Mandelkow *et al*., 1991; O'Toole *et al*., 1999). Therefore, microtubule dynamics in yeast is likely restricted to plus-ends. Fluorescence speckle microscopy studies find no evidence for minus-end assembly or disassembly of either polar microtubules in anaphase or astral microtubules (Maddox *et al*., 2000). Recent in vivo and in vitro studies find that Stu2p and XMAP215 act specifically at microtubule plus-ends to promote dynamicity (Kosco *et al*., 2001; Shirasu-Hiza *et al*., 2003; Van Breugal *et al*., 2003). Furthermore, Stu2p's spindle pole localization (minus-end proximal) is not surprising given that spindle pole components affect astral microtubule dynamics (Vogel *et al*., 2001). Therefore, we speculate that Stu2p can be regulated or stored by spindle poles before being shuttled to microtubule plus-ends to promote dynamics. Similar mechanisms have been described for loading Kar9p on cytoplasmic microtubules to facilitate proper spindle positioning (Liakopoulos *et al*., 2003). XMAP215 displays both stabilizing and destabilizing activity under varying experimental conditions (Gard and Kirschner, 1987; Vasquez *et al*., 1994; Popov *et al*., 2001; Shirasu-Hiza *et al*., 2003; Van Breugal *et al*., 2003). Stu2p may function differentially at plus-ends near the spindle pole to promote growth events and at plus-ends near the spindle equator to promote catastrophe events, thereby creating a gradient of microtubule polymerization and depolymerization. Gradients of microtubule regulation have been predicted by modeling experiments in budding yeast (Sprague

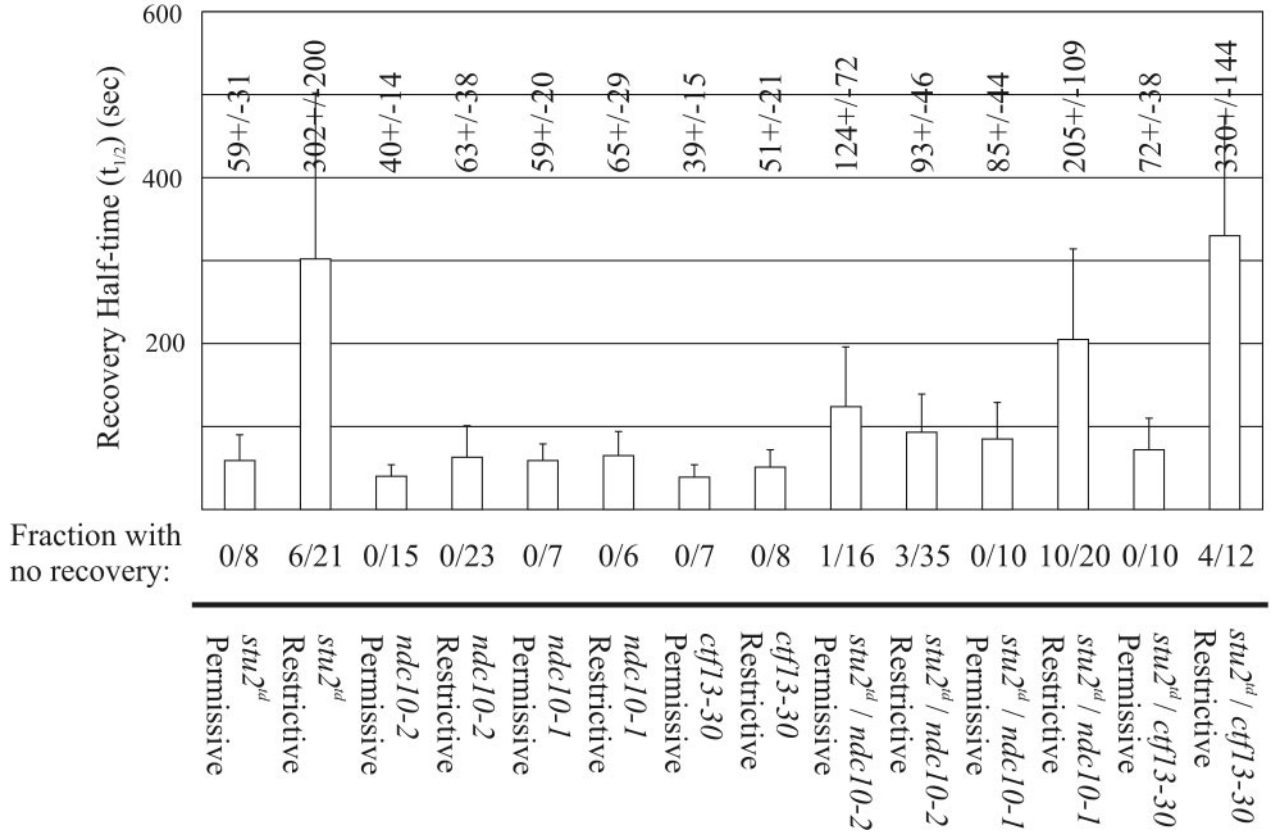

Figure 9. Kinetochore contribution to spindle microtubule dynamics. Comparison of $t_{1/2}$ values of bleached spindle microtubule tufts for *stu2^{td}*, *ndc10-2*, *ndc10-1*, *ctf13-30*, *ndc10-2/stu2^{td}*, *ndc10-1/stu2^{td}*, and *ctf13-30/stu2^{td}*. Experiments with no recovery (normalized recovery <16%) were not included in the recovery analysis. Recovery of spindle microtubule turnover was observed in *ndc10-2/stu2^{td}* double mutants but not in *ndc10-1/stu2^{td}* or *ctf13-30/stu2^{td}* cells.

et al., 2003) and experimental evidence in *Xenopus* extract systems (Kalab *et al.*, 2002). It is unlikely that microtubule turnover is due to attachment and detachment of microtubules to kinetochores. Once sister centromeres separate, their reassociation is infrequent, indicating that a gain and loss of tension between sister chromatids does not occur as would be expected for attachment and detachment (Goshima and Yanagida, 2001; Pearson *et al.*, 2001). Thus, we favor the model describing microtubule plus-end dynamics to be responsible for spindle microtubule turnover. The nature of Stu2p regulation of microtubule plus-end dynamics and the mechanism of spindle microtubule turnover will be the focus of important future research.

Functional Differences between Kinetochore Mutations

Both *ndc10-1* and *ndc10-2* disrupt proper segregation of the genome (Goh and Kilmartin, 1993; Kopski and Huffaker, 1997). Furthermore, *ndc10-1* disrupts centromere tension, localization of all kinetochore proteins tested and spindle assembly checkpoint function (Tavormina and Burke, 1998; Goshima and Yanagida, 2000; He *et al.*, 2000). We find that *ndc10-2* mutants are not as severe in their mislocalization of a core kinetochore component (Cse4p) compared with *ndc10-1*. Similarly, the two alleles were found to have different effects on the spindle assembly checkpoint. *ndc10-2* mutants exhibit an increased cell cycle delay in microtubule destabilizing drugs compared with *ndc10-1*, indicating that *ndc10-2* mutants are more competent than *ndc10-1* to activate the checkpoint (Burke, personal communication). Finally, our sequencing analysis shows that the *ndc10-2* (*A914T*) mutation is a single amino acid transition resulting in the substitution of a hydrophobic alanine residue to a hydrophilic threonine residue. The more functionally severe mutation (*ndc10-1; Q944**) is a 12-amino acid truncation also in the C terminus (our results, Burke and Kilmartin, personal communication). Thus, a kinetochore mutation causing a subtle change in microtubule dynamics (*ndc10-2*) is a partial kinetochore mutation, whereas the mutation without a measurable effect on microtubule dynamics (*ndc10-1*) results in complete kinetochore disruption. Furthermore, the close proximity of the two mutations suggests the carboxy terminal domain of *NDC10* is essential for regulation of kinetochore function.

Kinetochore Mutation That Promotes Microtubule Dynamics in the Absence of Stu2p: Evidence for Kinetochore Regulation of Microtubule Dynamics

stu2^{td} /ndc10-2 double mutants exhibited spindle microtubule dynamics that were significantly faster than *stu2^{td}* alone. Thus, kinetochores can regulate microtubules independent of Stu2p. The increased microtubule dynamics may be due to an altered state of microtubule attachment with a partially functional kinetochore. We infer the rescue of mi-

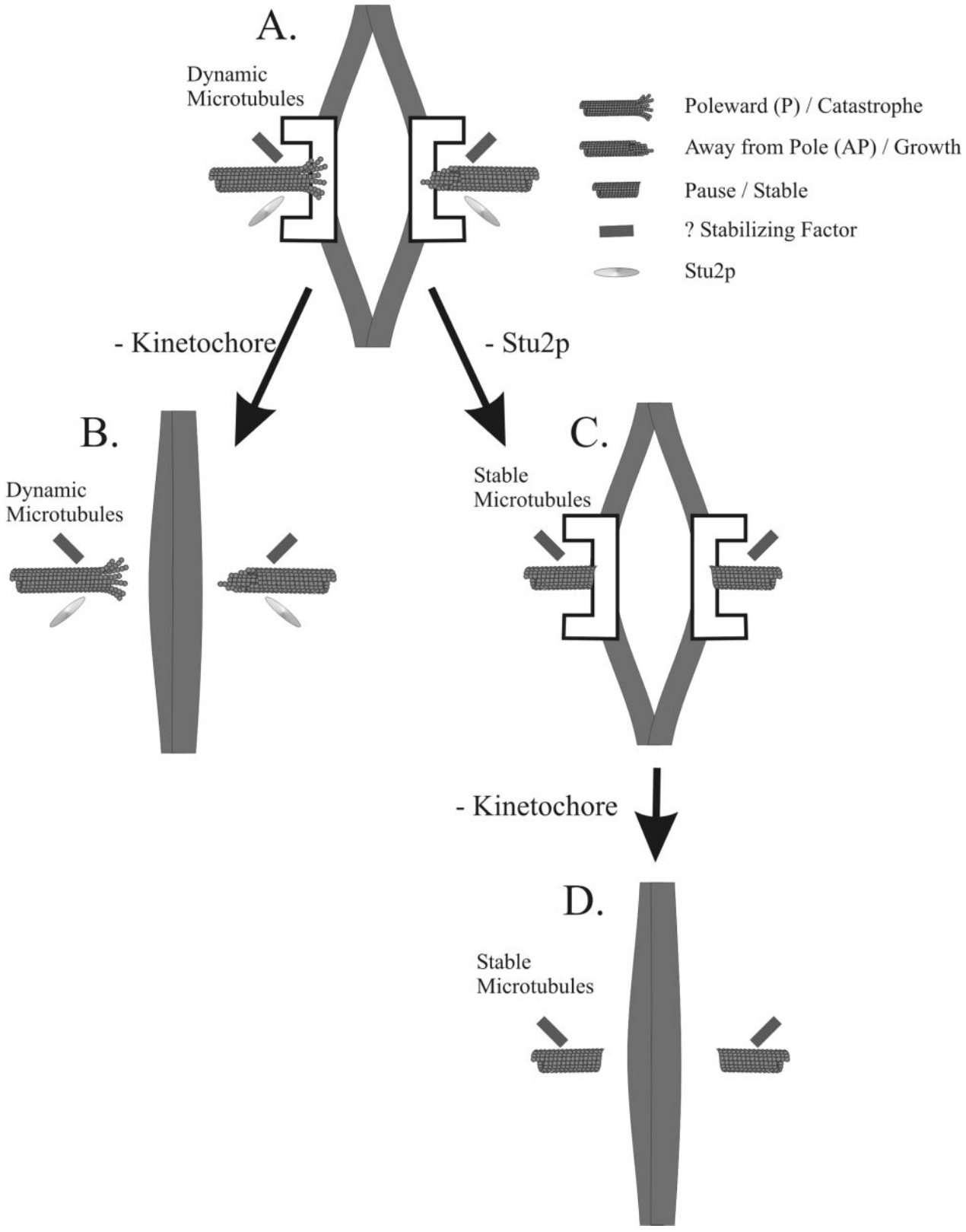

Figure 10. Model for regulation of spindle microtubule dynamics. (A) Dynamic spindle microtubules promoted by Stu2p are coupled to the force necessary for centromere oscillations. (B) Complete disruption of the kinetochore does not affect dynamics promoted by Stu2p. (C) Depletion of Stu2p stabilizes microtubules and centromere dynamics with separated sister centromeres indicating that kinetochores remain attached and under tension and Stu2p prevents the paused state of microtubule dynamics. (D) Complete disruption of the kinetochore without Stu2p causes stable microtubules, indicating that microtubule stabilization does not require the kinetochore.

crotubule turnover is due to a change in Ndc10p function at the kinetochore. However, we cannot rule out the possibility that Ndc10p functions at unattached microtubule plus-ends. *ndc10-2* kinetochores may generate dynamics by recruiting and/or allowing accessibility of other microtubule dynamics regulators or by limiting access of stabilization factors to the microtubule plus-end. In contrast to *ndc10-1*, *ndc10-2* single mutants seem to have partial kinetochore function to generate an altered state of dynamic microtubules. The rate of fluorescence recovery of $stu2^{td}$ */ndc10-2* spindles is not significantly different from *ndc10-2* alone, indicating that Stu2p is not necessary for promoting microtubule dynamics in *ndc10-2*.

These results provide evidence for a model where Stu2p promotes dynamics of free or attached microtubule plus-ends within the cell (Figure 10, C and D). Kinetochores are able to maintain attachment to growing, shortening, or paused microtubule plus-ends (evidenced by oscillations toward and away from the spindle pole). However, paused ends may not allow capture, orientation, error-correction mechanisms, or segregation. Therefore, dynamic plus-ends are the preferred physiological state; Stu2p's role in these processes is essential. In contrast, kinetochores are not required for microtubule dynamics. However, kinetochores must maintain attachment to plus-ends to sustain sister centromere oscillations. The discovery that *ndc10-2* promotes microtubule dynamics in the absence of Stu2p reveals kinetochore-specific regulation of microtubule dynamics to facilitate proper centromere positioning. The kinetochore specific mechanism may reflect local control of microtubule dynamics embedded in a kinetochore by limiting the access or activity of microtubule-stabilizing factors and thereby generating dynamic microtubules. Our results provide the first molecular evidence for separating the control of microtubule dynamics from kinetochore-specific regulation of individual kinetochore microtubules during mitosis.

ACKNOWLEDGMENTS

We thank E. Yeh, J. Deluca, J.C. Labbé, M. Karthikeyan, A. Desai and A. Hyman for stimulating discussions and wonderful support; D. Burke and J. Kilmartin for communicating unpublished results; K. Kosco and T. Huffaker for yeast strains; R. Heil-Chapdelaine, J. Cooper, T. Huffaker, A. Goldstein, J. McCusker, and the Yeast Resource Center for plasmids; and members of the Bloom laboratory for helpful and critical comments on the manuscript. This work was supported by National Institutes of Health grant GM-32238 to K.S.B and GM-24364 to E.D.S.

REFERENCES

Andersen, S.S., and Wittmann, T. (2002). Toward reconstitution of in vivo microtubule dynamics in vitro. Bioessays *24*, 305–307.

Belmont, A.S. (2001). Visualizing chromosome dynamics with GFP. Trends Cell Biol. *11*, 250–257.

Byers, B., Shriver, K., and Goetsch, L. (1978). The role of spindle pole bodies and modified microtubule ends in the initiation of microtubule assembly in *Saccharomyces cerevisiae.* J. Cell Sci. *30*, 331–352.

Chen, Y., Baker, R.E., Keith, K.C., Harris, K., Stoler, S., and Fitzgerald-Hayes, M. (2000). The N terminus of the centromere H3-like protein Cse4p performs an essential function distinct from that of the histone fold domain. Mol. Cell. Biol. *20*, 7037–7048.

Dhamodharan, R., Jordan, M., Thrower, D., Wilson, L., and Wadsworth, P. (1995). Vinblastine suppresses dynamics of individual microtubules in living cells. Mol. Biol. Cell *6*, 1215–1229.

Dogterom, M., and Yurke, B. (1997). Measurement of the force-velocity relation for growing microtubules. Science *278*, 856–860.

Doheny, K.F., Sorger, P.K., Hyman, A.A., Tugendreich, S., Spencer, F., and Hieter, P. (1993). Identification of essential components of the *S. cerevisiae* kinetochore. Cell *73*, 761–74.

Dohmen, R.J., Wu, P., and Varshavsky, A. (1994). Heat-inducible degron: a method for constructing temperature-sensitive mutants. Science *263*, 1273–1276.

Gard, D.L., and Kirschner, M.W. (1987). A microtubule-associated protein from *Xenopus* eggs that specifically promote assembly at the plus-end. J. Cell Biol. *105*, 2203–2215.

Goh, P.Y., and Kilmartin, J.V. (1993). *NDC10*: a gene involved in chromosome segregation in *Saccharomyces cerevisiae*. J. Cell Biol. *121* 503–512.

Goldstein, A.L., and McCusker, J.H. (1999). Three new dominant drug resistance cassettes for gene disruption in *Saccharomyces cerevisiae.* Yeast *15*, 1541–1553.

Goshima, G., and Yanagida, M. (2000). Establishing biorientation occurs with precocious separation of the sister kinetochores, but not the arms, in the early spindle of budding yeast. Cell *100*, 619–633.

Goshima, G., and Yanagida, M. (2001). Time course analysis of precocious separation of sister centromeres in budding yeast: continuously separated or frequently reassociated? Genes Cells *6*, 765–773.

He, X., Asthana, S., and Sorger, P.K. (2000). Transient sister chromatid separation and elastic deformation of chromosomes during mitosis in budding yeast. Cell *101*, 763–775.

He, X., Rines, D.R., Espelin, C.W., Sorger, P.K. (2001). Molecular analysis of kinetochore-microtubule attachment in budding yeast. Cell *106*, 195–206.

Hunt, A.J., and McIntosh, J.R. (1998). The dynamic behavior of individual microtubules associated with chromosomes in vitro. Mol. Biol. Cell *9*, 2857–2871.

Hyman, A.A., and Sorger, P.K. (1995). Structure and function of kinetochores in budding yeast. Annu. Rev. Cell Dev. Biol. *11*, 471–495.

Inoue, S., and Salmon, E.D. (1995). Force generation by microtubule assembly/disassembly in mitosis and related movements. Mol. Biol. Cell *6*, 1619–1640.

Jiang, W., Lechner, J., and Carbon, J. (1993). Isolation and characterization of a gene (CBF2) specifying a protein component of the budding yeast kinetochore. J. Cell Biol. *121*, 513–519.

Kalab, P., Weis, K., and Heald, R. (2002). Visualization of a Ran-GTP gradient in interphase and mitotic *Xenopus* egg extracts. Science *295*, 2452–2456.

Kapoor, T.M., and Compton, D.A. (2002). Searching for the middle ground: mechanisms of chromosome alignment during mitosis J. Cell Biol. *157*, 551–556.

Khodjakov,A.,Gabashvili,I.S.,andRieder,C.L.(1999)."Dumb"versus"smart"kinetochore models for chromosome congression during mitosis in vertebrate somatic cells. Cell Motil. Cytoskeleton *43*, 179–185.

Kinoshita, K., Arnal, I., Desai, A., Drechsel, D.N., and Hyman, A.A. (2001). Reconstitution of physiological microtubule dynamics using purified components. Science *294*, 1340–1343.

Kinoshita, K., Habermann, B., and Hyman, A.A. (2002). XMAP *215*, a key component of the dynamic microtubule cytoskeleton. Trends Cell Biol. *12*, 267–273.

Kopski, K.M., and Huffaker, T.C. (1997). Suppressors of the *ndc10–2* mutation: a role for the ubiquitin system in *Saccharomyces cerevisiae* kinetochore function. Genetics *147*, 409–420.

Kosco, K.A., Pearson, C.G., Maddox, P.S., Wang, P.J., Adams, I.R., Salmon, E.D., Bloom, K., and Huffaker, T.C. (2001). Control of microtubule dynamics by Stu2p is essential for spindle orientation and metaphase chromosome alignment in yeast. Mol. Biol. Cell *12*, 2870–2880.

Liakopoulos, D., Kusch, J., Grava, S., Vogel, J., and Barral, Y. (2003). Asymmetric loading of Kar9 onto spindle poles and microtubules ensures proper spindle alignment. Cell *112*, 561–574.

Longtine, M.S., Mckenzie Iii, A., Demarini, D.J., Shah, N.G., Wach, A., Brachat, A., Philippsen, P., and Pringle, J.R. (1998). Additional modules for versatile and economical PCR-based gene deletion and modification in *Saccharomyces cerevisiae.* Yeast *14*, 953–961.

Maddox, P., Bloom, K., and Salmon, E.D. (2000). Polarity and dynamics of microtubule assembly in the budding yeast *Saccharomyces cerevisiae.* Nat. Cell Biol. *2*, 36–41.

Mandelkow, E.M., Mandelkow, E., and Milligan, R.A. (1991). Microtubule dynamics and microtubule caps: a time-resolved cryo-electron microscopy study. J. Cell Biol. *114*, 977–991.

Marshall, W.F., Straight, A., Marko, J.F., Swedlow, J., Dernberg, A., Belmont, L., Murray, A.W., Agard, D.A., and Sedat, J.W. (1997). Interphase chromosomes undergo constrained diffusional motion in living cells. Curr. Biol. *7*, 930–939.

McIntosh, J.R., Grishchuk, E.L., and West, R.R. (2002). Chromosome-microtubule interactions during mitosis. Annu. Rev. Cell Dev. Biol. *18*, 193–219.

Mitchison, T., Evans, L., Schulze, E., and Kirschner, M. (1986). Sites of microtubule assembly and disassembly in the mitotic spindle. Cell *45*, 515–527.

Mitchison, T.J., and Salmon, E.D. (1992). Poleward kinetochore fiber movement occurs during both metaphase and anaphase-A in newt lung-cell mitosis. J. Cell Biol. *119*, 569–582.

Mitchison, T.J. (1989). Polewards microtubule flux in the mitotic spindle: evidence from photoactivation of fluorescence. J. Cell Biol. *109*, 637–652.

Murray, A.W., and Mitchison, T.J. (1994). Mitosis. Kinetochores pass the IQ test. Curr. Biol. *4*, 38–41.

Nabeshima, K., Nakagawa, T., Straight, A.F., Murray, A., Chikashige, Y., Yamashita, Y.M., Hiraoka, Y., and Yanagida, M. (1998). Dynamics of centromeres during metaphase-anaphase transition in fission yeast: Dis1 is implicated in force balance in metaphase bipolar spindle. Mol. Biol. Cell *9*, 3211–3225.

Nicklas, R.B. (1989). The motor for poleward chromosome movement in anaphase is in or near the kinetochore. J. Cell Biol. *109*, 2245–2255.

O'Toole, E.T., Winey, M., and McIntosh, J.R. (1999). High-voltage electron tomography of spindle pole bodies and early mitotic spindles in the yeast *Saccharomyces cerevisiae.* Mol. Biol. Cell *10*, 2017–2031.

Pearson, C.G., Maddox, P.S., Salmon, E.D., and Bloom, K. (2001). Budding yeast chromosome structure and dynamics during mitosis. J. Cell Biol. *152*, 1255–1266.

Popov, A.V., Pozniakovsky, A., Arnal, I., Antony, C., Ashford, A.J., Kinoshita, K., Tournebize, R., Hyman, A.A., and Karsenti, E. (2001). XMAP215 regulates microtubule dynamics through two distinct domains. EMBO J. *20*, 397–410.

Rieder, C.L., and Salmon, E.D. (1998). The vertebrate cell kinetochore and its roles during mitosis. Trends Cell Biol. *8*, 310–318.

Scholey, J.M., Brust-Mascher, I., and Mogilner, A. (2003). Cell division. Nature *422*, 746–752.

Severin, F., Habermann, B., Huffaker, T., and Hyman, T. (2001). Stu2 promotes mitotic spindle elongation in anaphase. J. Cell Biol. *153*, 435–442.

Shaw, S.L., Yeh, E., Bloom, K., and Salmon, E.D. (1997). Imaging green fluorescent protein fusion proteins in *Saccharomyces cerevisiae.* Curr. Biol. *7*, 701–704.

Shirasu-Hiza, M., Coughlin, P., and Mitchison, T. (2003). Identification of XMAP215 as a microtubule-destabilizing factor in *Xenopus* egg extract by biochemical purification. J. Cell Biol. *161*, 349–358.

Skibbens, R.V., Skeen, V.P., and Salmon, E.D. (1993). Directional instability of kinetochore motility during chromosome congression and segregation in mitotic newt lung cells: a push-pull mechanism. J. Cell Biol. *122*, 859–875.

Skoufias, D.A., Andreassen, P.R., Lacroix, F.B., Wilson, L., and Margolis, R.L. (2001). Mammalian mad2 and bub1/bubR1 recognize distinct spindle-attachment and kinetochore-tension checkpoints. Proc. Natl. Acad. Sci. USA *98*, 4492–4497.

Sprague, B.L., Pearson, C.G., Maddox, P.S., Bloom, K.S., Salmon, E.D., and Odde, D.J. (2003). Mechanisms of microtubule-based kinetochore positioning in the yeast metaphase spindle. Biophys. J. *84*, 3529–3546.

Straight, A.F., Marshall, W.F., and Murray, A.W. (1997). Mitosis in living budding yeast: anaphase A but no metaphase plate. Science *277*, 574–578.

Tanaka, T., Fuchs, J., Loidl, J., and Nasmyth, K. (2000). Cohesin ensures bipolar attachment of microtubules to sister centromeres and resists their precocious separation. Nat. Cell Biol. *2*, 492–499.

Tavormina, P.A., and Burke, D.J. (1998). Cell cycle arrest in cdc20 mutants of *Saccharomyces cerevisiae* is independent of Ndc10p and kinetochore function but requires a subset of spindle checkpoint genes. Genetics *148*, 1701–1713.

Toso, R.J., Jordan, M.A., Farrell, K.W., Matsumoto, B., and Wilson, L. (1993). Kinetic stabilization of microtubule dynamic instability in vitro by vinblastine. Biochemistry *32*, 1285–1293.

Tran, P.T., Walker, R.A., and Salmon, E.D. (1997). A metastable intermediate state of microtubule dynamic instability that differs significantly between plus and minus ends. J. Cell Biol. *138*, 105–117.

Van Breugal, M., Drechsel, D., and Hyman, A. (2003). Stu2p, the budding yeast member of the conserved Dis1/XMAP215 family of microtubule-associated proteins is a plus end-binding microtubule destabilizer. J. Cell Biol. *161*, 359–369.

Vasquez, R.J., Gard, D.L., and Cassimeris, L. (1994). XMAP from *Xenopus* eggs promotes rapid plus end assembly of microtubules and rapid microtubule polymer turnover. J. Cell Biol. *127*, 985–993.

Vasquez, R.J., Howell, B., Yvon, A.M., Wadsworth, P., and Cassimeris, L. (1997). Nanomolar concentrations of nocodazole alter microtubule dynamic instability in vivo and in vitro. Mol. Biol. Cell *8*, 973–985.

Vogel, J., Drapkin, B., Oomen, J., Beach, D., Bloom, K., and Snyder, M. (2001). Phosphorylation of gamma-tubulin regulates microtubule organization in budding yeast. Dev. Cell *1*, 621–631.

Wach, A., Brachat, A., Pohlmann, R., and Philippsen, P. (1994). New heterologous modules for classical or PCR-based gene disruptions in *Saccharomyces cerevisiae.* Yeast *10*, 1793–1808.

Wadsworth, P., and Salmon, E.D. (1988). Spindle microtubule dynamics: modulation by metabolic inhibitors. Cell Motil. Cytoskeleton *11*, 97–105.

Winey, M., Mamay, C.L., O'Toole, E.T., Mastronarde, D.N., Giddings, T.H., Jr., McDonald, K.L., and McIntosh, J.R. (1995). Three-dimensional ultrastructural analysis of the *Saccharomyces cerevisiae* mitotic spindle. J. Cell Biol. *129*, 1601–1615.

Winey, M., and O'Toole, E.T. (2001). The spindle cycle in budding yeast. Nat. Cell Biol. *3*, E23–E27.

Zhai, Y., Kronebusch, P.J., and Borisy, G.G. (1995). Kinetochore microtubule dynamics and the metaphase-anaphase transition. J. Cell Biol. *131*, 721–734.